# Accepted Manuscript

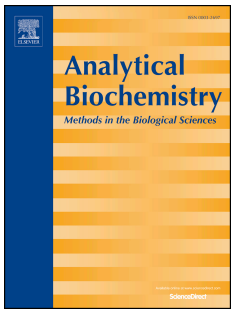


An ultrasensitive electrochemical genosensor for *Brucella* based on palladium nanoparticles

A. Rahi, N. Sattarahmady, H. Heli

PII: S0003-2697(16)30179-8

DOI: 10.1016/j.ab.2016.07.012

Reference: YABIO 12446

To appear in: *Analytical Biochemistry*

Received Date: 4 June 2016

Revised Date: 6 July 2016

Accepted Date: 11 July 2016

Please cite this article as: A. Rahi, N. Sattarahmady, H. Heli, An ultrasensitive electrochemical genosensor for *Brucella* based on palladium nanoparticles, *Analytical Biochemistry* (2016), doi: 10.1016/j.ab.2016.07.012.

# An ultrasensitive electrochemical genosensor for *Brucella* based on palladium nanoparticles

A. Rahi [a], N. Sattarahmady [a, b*], H. Heli [a]*

[a] Nanomedicine and Nanobiology Research Center, Shiraz University of Medical Sciences, Shiraz, Iran.

[b] Department of Medical Physics, School of Medicine, Shiraz University of Medical Sciences, Shiraz, Iran.

*Corresponding author. E-mail: sattarahmady@yahoo.com, nsattar@sums.ac.ir (N. Sattarahmady); hheli7@yahoo.com, heli@sums.ac.ir (H. Heli), Tel/Fax: +98 71 32 34 93 32.

## Abstract

Palladium nanoparticles were potentiostatically electrodeposited on a gold surface at a highly negative potential. The nanostructure, as a transducer, was utilized to immobilize a *Brucella*-specific probe and the process of immobilization and hybridization was detected by electrochemical methods. The proposed method for detection of the complementary sequence and a non-complementary sequence was applied. The fabricated genosensor was evaluated for the assay of the bacteria in the cultured and human samples with and without PCR. The genosensor could detect the

complementary sequence with a sensitivity of 0.02 μA $dm^3$ $mol^{-1}$, a linear concentration range of $1.0\times10^{-12}$ to$1.0\times10^{-19}$ mol $dm^{-3}$, and a detection limit of $2.7\times10^{-20}$ mol $dm^{-3}$.

*Keywords:* Palladium; Nanoparticles; Genosensor; *Brucella*; DNA biosensor

## 1. Introduction

DNA hybridization detection is a key parameter in the diagnosis of genetic diseases and pathogen agents. Various techniques such as immunoassays, surface plasmon resonance spectroscopy, quartz crystal microbalance, UV-vis spectroscopy [1-3] and electrochemical methods [4, 5] have been developed based on the DNA hybridization detection. Electrochemical genosensors are one of the best choices for development of sensitive, specific, simple and inexpensive devices for disease diagnosis [6].

Brucellosis is an infectious disease caused by the gram-negative bacteria of the genus *Brucella* with an intracellular life cycle. Brucellosis infections are almost invariably transmitted to people by contact with animals or animal products that are contaminated with these bacteria [7]. *Brucella* organisms are also biological warfare agents [8]. The etiological agents of brucellosis are various *Brucella* species.

Bacterial culture is the important part in confirmation of the presence of this disease [9]. However, the growth rate of the bacterium is slow and fastidious leading to misleading results [10] with low sensitivity [11]; it is time consuming and poses a risk for laboratory personnel [12, 13]. Other techniques have also been developed for brucellosis diagnosis such as complement fixation test (CFT), serum agglutination test (SAT), Rose Bengal plate test (RBT) [14, 15], PCR, rtPCR and qPCR [16-18], up-converting phosphor

technology-based lateral flow strip [19], monoclonal antibody-based assay [20], ELISA [21], real-time quantitative loop-mediated isothermal amplification assay (LAMP) [22], Raman spectroscopy [23], and serological tests [24]. Serological techniques suffer from serological cross-reactions [25, 26], low sensitivity in the acute phase, low specificity and high prevalence of Brucella-specific antibodies in epidemic areas of brucellosis. PCR-based methods have been limitedly employed in human samples [27], need more expensive equipment, and suffer from difficulty in the direct detection of PCR products [19]. The LAMP method also needs six primers and gel electrophoresis step using intercalating dyes or fluorescent tags. Moreover, most of these methods have problems associated with them such as requiring sophisticated procedures, being time consuming and needing trained personnel. In addition, these methods are only adapted for the qualitative or semi-quantitative detection for *Brucella* assays, which do not meet the requirements for the rapid and accurate identification of brucellosis in a shorter time; it delays the introduction of efficient remedial measures. Some immunosensors for detection of *Brucella* have also been reported [28, 29]. However, most of these sensors are label-dependent and require labeling of biomolecules to convert the antibody/antigen interaction into detectable (optical or electrochemical) signals. Therefore, development of rapid, inexpensive, and easy-to-use methodologies for direct detection of *Brucella* directly in real samples has attracted considerable interest.

Applications of nanomaterials in biosensing provide the advantages of high surface area of the transducers, enhanced electronic properties and amplified readout systems, and electrocatalytic and biocompatibile surfaces [30-34]. Palladium nanoparticles have

thermal stability, chemical inertness and affinity for the thiol groups, and can be used as a sensing platform in genosensor fabrication.

In the present study, an electrochemical label-free genosensor was developed based on palladium nanoparticles as a transducer for a rapid, simple and quantitative detection of *Brucella* organism in clinical samples.

## 2. Materials and methods

### *2.1. Materials*

All chemicals were of analytical grade from Scharlau (Spain) or Sigma (USA) and were used without further purification. All solutions were prepared by redistilled water. A thiolated oligonucleotide probe (probe oligonucleotide, p-ssDNA) was designed based on the common genomic sequence in all the *Brucella* species. The probe sequence was checked for any possible homology and share sequences with any non-*Brucella* species. Moreover, the melting temperature of the probe was ensured to be within a narrow range using Oligo software. Then, the probe sequence was checked for potential self-dimmer and formation of secondary structures using mfold software which may otherwise hinder the assay. p-ssDNA was ordered from Vivantis (Malaysia). A complementary-sequence oligonucleotide (target oligonucleotide, t-ssDNA) and non-complementary sequence oligonucleotide (nc-ssDNA) were purchased from SinaClon BioScience Co. (Iran). The oligonucleotide sequences are as follows:

p-ssDNA sequence: 5' SH-$(CH_3)_6$ TGC CGA TCA CTT AAG GGC CTT CAT 3';

t-ssDNA sequence: 5'-ATG AAG GCC CTT AAG TGA TCG GCA-3'

nc-ssDNA sequence: 5'-AGA CCA AAA AGG CCA CCC CCG GGT-3'

The oligonucleotide stock solutions were prepared with 20 mmol $dm^{-3}$ Tris-HCl buffer, pH 7.4 solution (Tris) and kept frozen.

*2.2. Apparatus*

Electrochemical measurements were carried out in a conventional three-electrode cell powered by a μ-Autolab potentiostat/galvanostat (the Netherlands). An Ag/AgCl, 3 mol $dm^{-3}$ KCl, a platinum wire, and a palladium nanoparticles-modified gold disk (nPd) electrode (2 mm of diameter) were used as the reference, counter and working electrodes, respectively. The system was run on a PC by GPES 4.9 software.

DNA samples for PCR amplification were extracted from *Brucella* strains, *Staphylococcus aureus* and *Klebsiella*. The PCR reaction was performed on an Eppendorf Mastercycler Gradient PCR system (USA). A solution of 50 mmol $dm^{-3}$ KCl, 10 mmol $dm^{-3}$ Tris-HCl (pH 9.0), 2 mmol $dm^{-3}$ $MgCl_2$, 200 μmol $dm^{-3}$ dNTPs, 20 pmol of each primers, and 2.5 IU Taq polymerase per 50 μL was employed. The primer sequences were as followed:

Forward primer: 5'-GACGAACGGAATTTTTCCAATCCC-3'

Reverse primer: 5'-TGCCGATCACTTAAGGGCCTTCAT-3'

For the IS711 assay, samples were cycled in a thermocycler with an initial denaturation at 95 °C for 5 min; this was followed by 35 cycles at 95 °C for 60 s, 60 °C for 60 s, and 72 °C for 60 s and one final extension at 72 °C for 3 min. Eight microliters of the amplification reaction mixture was taken and fractionated in a 2% agarose gel containing TBE buffer (100 mmol $dm^{-3}$ Tris-HCl (pH 8.0), 90 mmol $dm^{-3}$ boric acid, 1 mmol $dm^{-3}$ Na-EDTA), stained with an ethidium bromide solution (0.5 g $dm^{-3}$), and

visualized under UV light. To measure the concentration of the extracted DNA samples, Thermo Scientific NanoDrop 2000c (USA) was employed.

Field emission scanning electron microscopy (FESEM) was performed using a Zeiss, Sigma-IGMA/VP (Germany). The samples were coated by a 2-5 nm thin film of gold through sputtering.

*2.3. Preparation of the modified electrode*

Before electrodeposition of palladium nanoparticles, the gold disk electrode was polished on a sand paper and then on a polishing pad with 50 nm-alumina powder lubricated by glycerin. Polishing was continued to attain a mirror-like gold surface. The electrode was then cleaned by immersion in a 1:3 water/ethanol mixture and ultrasonication for 8 min in an ultrasound bath. The gold disk electrode was then placed in the cell containing the synthesis solutions comprising 15 mmol $dm^{-3}$ $PdCl_2$ in 1.0 mol $dm^{-3}$ $H_2SO_4$. Electrodeposition of palladium nanoparticles was performed at -4 V for 20 s in the stationary synthesis solution. The nPd electrode was then rinsed thoroughly with distilled water.

*2.4. Immobilization of 6-Mercapto-1-hexanol (MCH) on nPd electrode surface*

Immobilization of MCH was performed by dropping 10.0 μL of 1.0 mmol $dm^{-3}$ MCH solution dissolved in Tris on the nPd electrode surface at room temperature for 30 min. Then the electrode (nPd-MCH) was rinsed with Tris and double distilled water, respectively, to remove unspecific absorbed MCH.

*2.5. Immobilization of p-ssDNA on nPd electrode surface*

Immobilization of p-ssDNA probe was performed by dropping 10.0 μL of 10.0 μmol $dm^{-3}$ p-ssDNA solution dissolved in Tris on the nPd electrode surface and kept refrigerated at 4 °C for 8 h [35]. Then the electrode was rinsed with Tris. The p-ssDNA-modified nPd electrode was further treated with 1.0 mmol $dm^{-3}$ 6-Mercapto-1-hexanol (MCH) at room temperature for 30 min to obtain a well aligned p-ssDNA monolayer [36]. Then the electrode was washed again with Tris and double distilled water, respectively, to remove unspecific absorbed p-ssDNA. The obtained electrode was denoted as the genosensor.

*2.6. Hybridization*

The hybridization process was performed by immersing the genosensor into Tris containing various concentrations of t-ssDNA for 1 h at 37 °C. Then, the electrode was rinsed with Tris to remove the un-hybridized t-ssDNA, and then it was incubated in a solution containing Tris + NaCl (20 mmol $dm^{-3}$) + methylene blue (MB, 20 μmol $dm^{-3}$) for 5 min at 37 °C [35, 37]. Finally, the electrode was rinsed with Tris to remove the physically absorbed MB.

*2.7. Electrochemical measurements*

The real surface area of the nPd electrode was measured electrochemically. The nPd electrode was transferred to a solution of KCl (0.5 mol $dm^{-3}$) containing $K_4[Fe(CN)_6]$ (0.5 mmol $dm^{-3}$) and cyclic voltammograms at different potential sweep rates were measured. Using the Randles-Sevcik equation [38] and the value of $7.60\times10^{-6}$ cm $s^{-1}$ for the

diffusion coefficient of $[Fe(CN)_6]^{4-}$ [39], we obtained the real surface area of the nPd electrode.

Electrochemical detection of the DNA hybridization was performed in an electrochemical cell containing 10 mL Tris by recording cyclic voltammograms (CVs) and differential pulse voltammograms (DPVs) for the reduction peak of intercalated MB. The parameters of DPV recording were pulse width of 25 mV, a pulse time of 50 ms, and a scan rate of 10 mV $s^{-1}$. The concentration of t-ssDNA was quantified as the MB reduction peak current.

*2.8. Bacteria culture, human samples, and genomic DNA extraction*

*Brucella* agar culture medium with the addition of 5% horse blood was used for the cultivation of *Brucella* organisms by incubation at 35±2 °C for 48-72 h.

11 human serum samples with Brucellosis (Wright and 2ME tests were positive in all samples) were provided from veterinary administration of Fars province. It should be noted that a healthy blood sample was evaluated with suspicious samples. From 11 human serum samples with Brucellosis, 4 were measured after amplification by PCR and 7 samples were measured without amplification. Before performing the required investigations, the genomes were placed for 5 min at 90 ° C.

**3. Results and discussion**

Fig. 1 shows the FESEM images of the palladium nanoparticles with different magnifications and the corresponding EDS spectra. The nanoparticles comprised pure palladium (the main detected element, the gold signal is due to the coating during the

sample preparation) and covered entire the surface. The nanoparticles have some flat surfaces and are not perfect spheres with a mean size of 46±15 nm (n=160).

The potential of the nPd electrode to immobilize alkanethiols was evaluated by modification of nPd electrode by MCH and its electron transfer ability toward redox reaction of MB. As it is presented in Fig. 2, MB represented a well define peak in DPV recorded using the nPd electrode, while its redox transition is relatively hindered by blocking the surface by MCH. MB does not have affinity to MCH, and MCH layer formed on the nPd electrode surface repel MB from the surface confirming formation of a self-assemble layer of MCH. Self-assemble formation of alkanethiols on palladium surface has also been previously reported [40-43]. Palladium has some advantages (compared to gold) due to smaller grain size of its films leading to low defective and edge roughness surface, compatibility with complementary metal oxide semiconductor processing, long term stability, catalytic nature, lower cost, stability and biocompatibility [44]. Monoloyers of alkanethiols on palladium surface are self-assembled on a palladium sulfide interphase, and formed a dense and highly oriented chain [44]. On the other hand, the real surface area for the nPd electrode was about 1.6 times of the gold disk electrode (the related data was presented in supplementary material S1). Therefore, the nPd electrode provides a suitable substrate for the fabrication of the genosensor. Scheme 1 represents the fabrication protocol of the genosensor and detection of t-ssDNA.

Fig. 3 shows DPVs of MB (as a redox marker) interacting with p-ssDNA before and after hybridization with different concentrations of t-ssDNA recorded in Tris. MB binds with ssDNA and dsDNA through different forces including electrostatic attractions and intercalation [45]. Under the ionic strength of the MB solution employed here, binding of

MB with the free guanine bases of p-ssDNA is favorable [46]. This binding is performed through hydrophobic forces between the aromatic rings in the structure of guanine and MB. While the peak current of DPV for nc-ssDNA is almost equal to p-ssDNA, the MB reduction peak current depends on the t-ssDNA concentration, as shown in Fig. 3, inset. The plot is linear with a regression equation of $y = -(0.4258\pm0.0098)x - (9.5511\pm0.1530)$ in the range of $1.0 \times10^{-12}$ to $1.0\times10^{-19}$ mol $dm^{-3}$ of t-ssDNA with a limit of detection (LOD, as 3SD/m) of $2.7\times10^{-20}$ mol $dm^{-3}$ of the *Brucella* gene sequence. A comparison between LOD values reported for the Brucella detection methods is presented in Table 1.

To verify the regeneration of the genosensor, it was hybridized with $1.0\times10^{-13}$ mol $dm^{-3}$ t-ssDNA, and then immersed in hot water of 90 °C for 5 min to de-hybridize the formed dsDNA. It was then re-hybridized with the same t-ssDNA concentration and this cycle was repeated five times. Fig. 4 shows the results. The peak currents in DPVs showed a RSD of 2.2% for the regeneration of the genosensor.

In order to detect the *Brucella* genomic DNA, the DNA genome was extracted from *Brucella abortus*, and the DNA concentrations in the extracted samples were determined. Then, solutions of bacterial genome with different concentrations were prepared. The solutions were placed at 90 °C for 5 minutes to de-hybridize. After that, DPVs for the solution were measured and the corresponding calibration curve was plotted (Fig. 5). Based on the obtained results, the genome of *Brucella* species can be detected with regression equation of $y = -(0.3911\pm0.0091)x - (4.5876\pm0.1520)$ and a LOD of $8.2\times10^{-20}$ mol $dm^{-3}$.

To evaluate the selectivity of the genosensor, nc-ssDNA and two other bacterial genomes of non-*Brucella* samples of *Staphylococcus aureus* and *Klebsiella* were checked

as negative controls. DNA genomes were extracted from these species, amplified by PCR, and de-hybridized. A concentration of 2.0 ng $\mu L^{-1}$ from these samples, and a concentration of $1.0 \times 10^{-13}$ mol $dm^{-3}$ from nc-ssDNA were analyzed with the genosensor. The results are presented in Fig. 6. For these species, the peak currents in DPVs showed slight decrements, compared to the peak current for the genosensor.

To apply the genosensor for detection of *Brucella* in brucellosis patients, human serum samples were analyzed with and without PCR amplifications. DNA was extracted from (11 patients and one healthy) human serum samples and 4 patient's samples were amplified by PCR. The samples were then de-hybridized, and analyzed using the genosensor. The PCR amplified samples had a concentration of $1.1 \times 10^{-6}$ ng $\mu L^{-1}$. While the peak currents in DPVs obtained using the genosensor for the healthy sample were almost the same as p-ssDNA, the PCR amplified patient's samples represented drastic decrements. Moreover, decrements in the peak currents for the un-amplified samples were >10×standard deviation of the peak current for p-ssDNA (n=10). Therefore, these decrements in the peak currents are significant and confirm the presence of *Brucella* in the un-amplified sample. The results indicated that this label-free genosensor is capable of detecting *Brucella* in the blood samples from patients and did not require the sample to be processed in any way.

The stability of the genosensor was explored by recording the peak current in DPVs for $1.0 \times 10^{-13}$ mol $dm^{-3}$ t-ssDNA, while the genosensor was stored in Tris in the refrigerator at 4 °C and measured in the same conditions (Fig. 7). No regular change was observed at least for 30 days.

## 4. Conclusion

- A simple electrodeposition method was employed to fabricate palladium nanoparticles at the surface.

-The nanoparticles were checked for the immobilization of a *Brucella*-specific thiolated probe, and the results indicated that palladium nanoparticles had a great potential to fabricate the genosensors using thiolated sensing elements.

- The fabricated label-free genosensor showed a high sensitivity to detect brucellosis in the real samples even without using PCR amplification.

## Acknowledgments

We would like to thank the Research Council of Shiraz University of Medical Sciences (9697), and the Iran National Science Foundation (INSF) for supporting this research.

## References

[1] N. Sattarahmady, G.H. Tondro, M. Gholchin, H. Heli, Gold nanoparticles biosensor of Brucella spp. genomic DNA: Visual and spectrophotometric detections, Biochem. Engin. J. 97 (2015) 1-7.

[2] N. Sattarahmady, Z. Kayani, H, Heli, Highly simple and visual colorimetric detection of Brucella melitensis genomic DNA in clinical samples based on gold nanoparticles, J. Iran Chem. Soc. 12 (2015) 1569-1576.

[3] N. Sattarahmady, A. Movahedpour, H. Heli, G.R. Hatam, Gold nanoparticles-based biosensing of Leishmania major kDNA genome: Visual and spectrophotometric detections, Sens. Actuate B, in press, DOI: 10.1016/j.snb.2016.05.023

[4] A.O. Brett, DNA-based biosensors, Compr. Anal. Chem. 44 (2005) 179-208.

[5] H. Heli, N. Sattarahmady, G.R. Hatam, F. Reisi, R. Dehdari Vais, An electrochemical genosensor for Leishmania major detection based on dual effect of immobilization and electrocatalysis of cobalt-zinc ferrite quantum dots, Talanta 156-157 (2016) 172-179.

[6] J.J. Gooding, Electrochemical DNA hybridization biosensors, Electroanalysis 14 (2002) 1149-1156.

[7] W.Y. Zhang, W.D. Guo, S.H. Sun, J.F. Jiang, H.L. Sun, S.L. Li, Human brucellosis, Inner. Mongolia China Emerg. Infect. Dis. 16 (2010) 2001-2003.

[8] F.P. Poester, K. Nielsen, L.E. Samartino, W.L. Yu, Diagnosis of brucellosis, Open Vet. Sci. J. 4 (2010) 46-60.

[9] S. Al Dahouk, L.D. Sprague, H. Neubauer, New developments in the diagnostic procedures for zoonotic brucellosis in humans, Rev. Sci. Tech. Off Int. Epiz. 32 (2013) 177-188.

[10] B.I. Batchelor, R.J. Brindle, G.F. Gilks, J.B. Selkon, Biochemical mis-identification of Brucella melitensis and subsequent laboratory-acquired infections, J. Hosp. Infect. 22 (1992) 159-162.

[11] P. Yagupsky, Detection of Brucellae in blood cultures, J. Clin. Microbiol. 37 (1999) 3437-3442.

[12] E. Navarro, M.A. Casao, J. Solera, Diagnosis of human brucellosis using PCR, Expert. Rev. Mol. Diagnos. 4 (2004) 115-123.

[13] B.J. Bricker, PCR as a diagnostic tool for brucellosis, Vet. Microbiol. 90 (2002) 435-446.

[14] S. Mitka, C. Anetakis, E. Souliou, E. Diza, A. Kansouzidou, Evaluation of different PCR assays for early detection of acute and relapsing brucellosis in humans in comparison with conventional methods, J. Clin. Microbiol. 45 (2007) 1211-1218.

[15] S. O'Leary, M. Sheahan, T. Sweeney, Brucella abortus detection by PCR Assay in blood, milk and lymph tissue of serologically positive cows, Res. Vet. Sci. 81 (2006) 170-176.

[16] C. Hänsel, K. Mertens, M.C. Elschner, F. Melzer, Novel real-time PCR detection assay for Brucella suis, Vet. Rec. Open 2 (2015) 84-87.

[17] L. Bounaadja, D. Albert, B. Chenais, S. Hénault, M.S. Zygmunt, S. Poliak, Real-time PCR for identification of Brucella spp.: a comparative study of IS711, bcsp31 and per target genes, Vet. Microbiol. 137 (2009) 156-164.

[18] E. Navarro, J. Escribano, J.A. Fernandez, J. Solera, Comparison of three different PCR methods for detection of Brucella spp. in human blood samples, FEMS Immun. Med. Microbiol. 34 (2002) 147-151.

[19] Q. Qu, Z. Zhu, Y. Wang, Z. Zhong, J. Zhao, F. Qiao, Rapid and quantitative detection of Brucella by up-converting phosphor technology-based lateral-flow assay, J. Microbiol. Methods 79 (2009) 121-123.

[20] F. Biancifiori, F. Garrido, K. Nielsen, L. Moscati, M. Duran, D. Gall, Assessment of a monoclonal antibody-based competitive enzyme linked immunosorbent assay

(cELISA) for diagnosis of brucellosis in infected and Rev.1 vaccinated sheep and goats, New Microbiol. 23 (2000) 399-406.

[21] J.A. McGiven, J. Sawyer, L.L. Perrett, S.D. Brew, N.J. Commander, A. Fisher, A new homogeneous assay for high throughput serological diagnosis of brucellosis in ruminants, J. Immun. Methods 337 (2008) 7-15.

[22] K. Karthik, R. Rathore, P. Thomas, T.R. Arun, K.N. Viswas, R.K. Agarwal, Loop-mediated isothermal amplification (LAMP) test for specific and rapid detection of Brucella abortus in cattle, Vet. Quart. 34 (2014) 174-179.

[23] S. Meisel, S. Stöckel, M. Elschner, F. Melzer, P. Rösch, J. Popp, Raman spectroscopy as a potential tool for detection of Brucella spp. in milk, Appl. Envir. Microbiol. 78 (2012) 5575-5583.

[24] C.M. Marin, D.B.M. Jiménez, J.M. Blasco, C. Gamazo, I. Moriyon, R. Diaz, Comparison of three serological tests for Brucella ovis infection of rams using different antigenic extracts, Vet. Rec. 125 (1989) 504-508.

[25] M. Doganay, B. Aygen, Human brucellosis: an overview, Int. J. Infect. Dis. 7 (2003) 173-182.

[26] P.M. Munoz, C.M. Marin, D. Monreal, D. Gonzalez, B. Garin-Bastuji, Efficacy of several serological tests and antigens for diagnosis of bovine brucellosis in the presence of false-positive serological results due to Yersinia enterocolitica O: 9, Clin. Diagnos. Lab Immun. 12 (2005) 141-151.

[27] L. Zerva, K. Bourantas, S. Mitka, A. Kansouzidou, N.J. Legakis, Serum is the preferred clinical specimen for diagnosis of human brucellosis by PCR, J. Clin. Microbiol. 39 (2001) 1661-1664.

[28] Y. Liebes, R.S. Marks, M. Banai, Chemiluminescent optical fiber immunosensor detection of brucella cells presenting smooth-A antigen, Sens. Actuat. B 140 (2009) 568-576.

[29] Z.Z. Li, F.C. Gong, G.L. Shen, R.Q. Yu, Bacteria-modified amperometric immunosensor for a brucella melitensis antibody assay, Anal. Sci. 18 (2002) 625-630.

[30] C. Parolo, A. de la Escosura-Muniz, A. Merkoci, Electrochemical DNA sensors based on nanoparticles, C. Serge (Eds), Electrochemical Biosensors, CRC Press, 2015, pp. 195-221.

[31] A. Rahi, N. Sattarahmady, H. Heli, Label-free electrochemical aptasensing of the human prostate-specific antigen using gold nanospears, Talanta 156-157 (2016) 218-224.

[32] H. Heli, O. Amirizadeh, Non-enzymatic glucose biosensor based on hyperbranched pine-like gold nanostructure, Mater. Sci. Eng. C 63 (2016) 150-154.

[33] H. Heli, J. Pishahang, H. Barzegar Amiri, Synthesis of hexagonal CoAl-layered double hydroxide nanoshales/carbon nanotubes composite for the non-enzymatic detection of hydrogen peroxide, J. Electroanal. Chem. 768 (2016) 134-144.

[34] A. Rahi, K. Karimian, H. Heli, Nanostructured materials in electroanalysis of pharmaceuticals, Anal. Biochem. 497 (2016) 39-47.

[35] A. Rahi, N. Sattarahmady, H. Heli, Zepto-molar electrochemical detection of Brucella genome based on gold nanoribbons covered by gold nanoblooms, Sci. Rep. 5 (2015) 18060.

[36] L. Wang, X. Chen, X. Wang, X. Han, S. Liu, C. Zhao, Electrochemical synthesis of gold nanostructure modified electrode and its development in electrochemical DNA biosensor, Biosens. Bioelectron. 30 (2011) 151-157.

[37] G.S. Bang, S. Cho, B.G. Kim, A novel electrochemical detection method for aptamer biosensors, Biosens. Bioelectron. 21 (2005) 863-870.

[38] A.J. Bard, L.R. Faulkner, Electrochemical Methods, John Wiley, New York, 2001, pp. 448.

[39] S.F.Wang, Q. Xu, Electrochemical parameters of ethamsylate at multi-walled carbon nanotube modified glassy carbon electrodes, Bioelectrochem. 70 (2007) 296-300.

[40] J.C. Love, D.B. Wolfe, R. Haasch, M.L. Chabinyc, K.E. Paul, G.M. Whitesides, Formation and structure of self-assembled monolayers of alkanethiolates on palladium, J .Am. Chem. Soc. 125 (2003) 2597-2609.

[41] A. Carvalho, M. Geissler, H. Schmid, B. Michel, E. Delamarche, Self-assembled monolayers of eicosanethiol on palladium and their use in microcontact printing, Langmuir 18 (2002) 2406-2412.

[42] T.R. Soreta, J. Strutwolf, C.K. O'Sullivan, Electrochemically Deposited Palladium as a Substrate for Self-Assembled Monolayers, Langmuir 23 (2007) 10823-10830.

[43] T.R. Soreta, J. Strutwolf, O. Henry, C.K. O'Sullivan, Electrochemical surface structuring with palladium nanoparticles for signal enhancement, Langmuir 26 (2010) 12293-12299.

[44] J.C. Love, L.A. Estroff, J.K. Kriebel, R.G. Nuzzo, G.M. Whitesides, Self-assembled monolayers of thiolates on metals as a form of nanotechnology, Chem. Rev. 105 (2005) 1103-1170.

[45] E. Farjami, L. Clima, K.V. Gothelf, E.E. Ferapontova, DNA interactions with a methylene blue redox indicator depend on the DNA length and are sequence specific, Analyst 135 (2010) 1443-1448.

[46] A. Mudasir, E.T. Wahyuni, D.H. Tjahjono, N. Yoshioka, H. Inoue, Spectroscopic studies on the thermodynamic and thermal denaturation of the ct-DNA binding of methylene blue, Spectrochim. Acta A 77 (2010) 528-34

[47] D. Metzgar, M. Frinder, R. Lovari, D. Toleno, C. Massire, L.B. Blyn, Broad-spectrum biosensor capable of detecting and identifying diverse bacterial and candida species in blood, J. Clin. Microbiol. 51 (2013) 2670-2678.

[48] J.A. Qasem, S. AlMomin, S.A. Al-Mouqati, V. Kumar, Characterization and evaluation of an arbitrary primed Polymerase Chain Reaction (PCR) product for the specific detection of Brucella species, Saudi J. Biol. Sci. 22 (2015) 220-226.

[49] A.S. Amin, M.E. Hamdy, A.K. Ibrahim, Detection of Brucella melitensis in semen using the polymerase chain reaction assay, Vet. Microbiol. 83 (2001) 37-44.

[50] G. Schmoock, R. Ehricht, F. Melzer, M. Elschner, H. Tomaso, H. Neubauer, S. Al Dahouk, Development of a diagnostic multiplex polymerase chain reaction microarray assay to detect and differentiate Brucella spp, Diagnos. Microbiol. Infect. Dis. 71 (2011) 341-353.

[51] A.K. Gupta, V.K. Rao, D.T. Selvam, A. Kumar, R. Jain, Amperometric immunosensor of Brucella abortus CE-protein antigen shows post-zone phenomena, J. Electroanal. Chem. 717 (2014) 83-89.

[52] D.T. Newby, T.L. Hadfield, F.F. Roberto, Real-time PCR detection of Brucella abortus: a comparative study of SYBR green I, 5' exonuclease, and hybridization probe sssays, Appl. Environ. Microbiol. 69 (2015) 4753-4759.

[53] N.E. Lucero, G.I. Escobar, S.M. Ayala, P.S. Paulo, K. Nielsen, Fluorescence polarization assay for diagnosis of human brucellosis, J. Med. Microbiol. 52 (2003) 883-887.

[54] Huelseweh B, Ehricht R, Marschall HJ. Novel real-time PCR detection assay for Brucella suis, Proteomics 6 (2006) 2972-2981.

[55] V. Hinic, I. Brodard, A. Thomann, M. Holub, R. Miserez, C. Abril, IS711-based real-time PCR assay as a tool for detection of Brucella spp. in wild boars and comparison with bacterial isolation and serology, BMC Vet. Res. 5 (2009) 22-26.

[56] B. Sumerkan, S. Gokahmetoglu, D. Esel, Brucella detection in blood: comparison of the BacT/Alert standard aerobic bottle, BacT/Alert FAN aerobic bottle and BacT/Alert enhanced FAN aerobic bottle in simulated blood culture, Clin. Microbiol. Infect. 7 (2001) 369-372.

[57] L. Song, J. Li, S. Hou, X. Li, S. Chen, Establishment of loop-mediated isothermal amplification (LAMP) for rapid detection of Brucella spp. and application to milk and blood samples, J. Microbiol. Methods 90 (2012) 292-297.

[58] M. Soleimani, S. Shams, A.K. Majidzadeh, Developing a real-time quantitative loop-mediated isothermal amplification assay as a rapid and accurate method for detection of Brucellosis, J. Appl. Microbiol. 115 (2013) 828-834.

**Figure legends:**

Fig. 1: FESEM images of the palladium nanoparticles with different magnifications and the corresponding EDS spectra.

Fig. 2: DPVs of MB recorded using the nPd and nPd-MCH electrodes in a solution of Tris + 20 mmol $dm^{-3}$ NaCl + 20 μmol $dm^{-3}$ MB.

Fig. 3: DPVs of MB interacting with the genosensor before (blue curve) and after (red curves) hybridization with different concentrations of t-ssDNA recorded in Tris. Inset: Dependency of the peak currents of DPV on the t-ssDNA concentration (the corresponding calibration curve).

Fig. 4: DPVs of MB for the regeneration of the genosensor. Blue curves indicate DPVs before hybridization, and red curves indicate DPVs of the genosensor after multiple hybridization with $1.0\times10^{-13}$ mol $dm^{-3}$ t-ssDNA.

Fig. 5: DPVs of MB interacting with the genosensor before (blue curve) and after (red curves) hybridization with different concentrations of *Brucella* genomic DNA recorded in Tris. Inset: Dependency of the peak currents of DPV on the *Brucella* genomic DNA concentration (the corresponding calibration curve).

Fig. 6: DPVs of MB interacting with p-ssDNA before, and after hybridization with $1.0\times10^{-13}$ mol $dm^{-3}$ t-ssDNA, $1.0\times10^{-13}$ mol $dm^{-3}$ nc-ssDNA, 2.0 ng $\mu L^{-1}$ *Staphylococcus aureus* genome, and 2.0 ng $\mu L^{-1}$ *Klebsiella*.

Fig. 7: Repetitive DPVs of MB interacting with the genosensor after hybridization with $1.0\times10^{-13}$ mol $dm^{-3}$ t-ssDNA recorded for 30 days. Inset: Dependency of the peak currents for DPVs presented in the main panel on time.

Scheme 1: Fabrication protocol of the genosensor and detection of t-ssDNA.

Table 1: A comparison between LOD values reported for the Brucella detection methods.

| Type | Detection method | LOD | Reference |
|---|---|---|---|
| Brucella neotomae | PCR/ESI-MS | 320 CFU $mL^{-1}$ | 47 |
| Brucella spp. | PCR | 1 ng $mL^{-1}$ | 48 |
| Brucella spp. | Visual, Spectrophotometry | 102.5 pg $\mu L^{-1}$, 1.36 pg $\mu L^{-1}$ | 1 |
| Brucella spp. | UPT-LF | $5\times10^{6}$ CFU $mL^{-1}$ | 19 |
| Brucella spp. | ELISA | diagnostic sensitivity>96% | 21 |
| Brucella abortus | Real-time PCR | $1\times10^{1}$ gene copies | 15 |
| Brucella melitensis | PCR | 100 CFU $mL^{-1}$ | 49 |
| Brucella canis, Brucella abortus, Brucella melitensis, Brucella ovis | Real-time PCR | 6, 7, 7, 38 copy numbers | 17 |
| Brucella spp. | Multiplex PCR microarray assay | 200 genome equivalents | 50 |
| Brucella abortus | Amperometric immunosensing | 0.1 μg $mL^{-1}$ | 51 |
| Brucella abortus | Real-time PCR | 10-100 fg bacterial genome | 52 |
| Brucella melitensis | Visual, Spectrophotometry | 170.8 pg $\mu L^{-1}$, 3.32 pg $\mu L^{-1}$ | 2 |
| Brucella spp. | Fluorescence polarization assay | diagnostic sensitivity=96.1% | 53 |
| Brucella suis | Real-time PCR | 12.5 fg $\mu L^{-1}$ | 16 |
| Brucella spp. | PCR[1] | 20 pg, 5 pg, 8 fg | 18 |
| Brucella melitensis | Protein array | $1\times10^{6}$ CFU $mL^{-1}$ | 54 |
| Brucella spp. | Real-time PCR | 10 gene copies | 55 |
| Brucella spp. | Blood culture bottles | $10^{2}$ microorganisms $g^{-1}$ feces | 56 |
| Brucella spp. | Loop-mediated isothermal amplification method | 3.81 CFU | 57 |
| Brucella spp. | Real-time loop-mediated isothermal amplification | 17 genome copies | 58 |
| Brucella spp. | Electrochemical genosensing | $2.7\times10^{-20}$ mol $dm^{-3}$ | This work |

PCR/ESI-MS: PCR paired with electrospray ionization-mass spectrometry
UPT-LF: Up-converting phosphor technology-based later-flow assay
1. Primers JPF/JPR, primers B4/B5, primers F4/R2

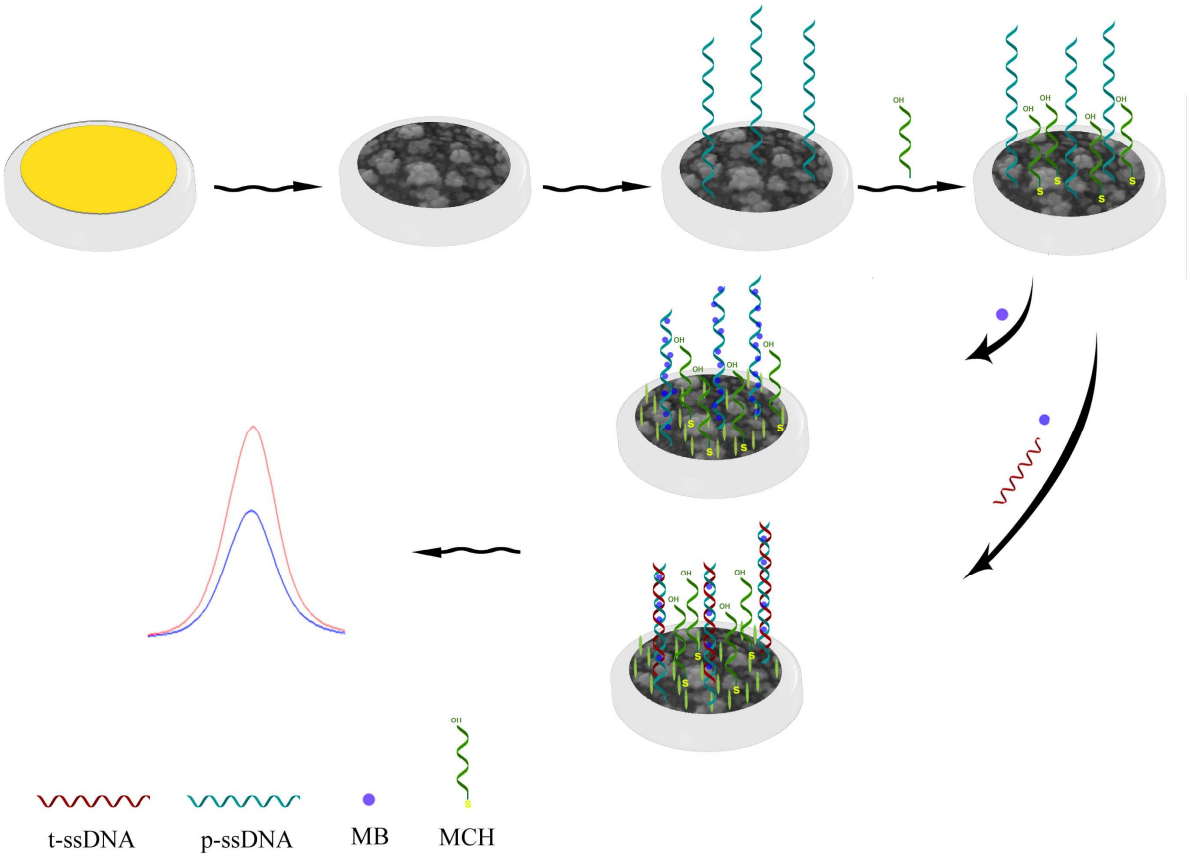

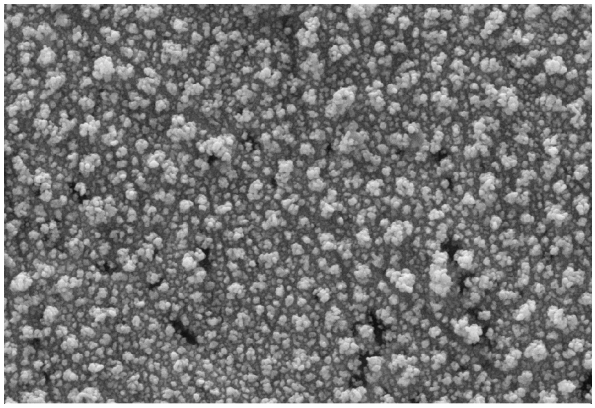
200 nm

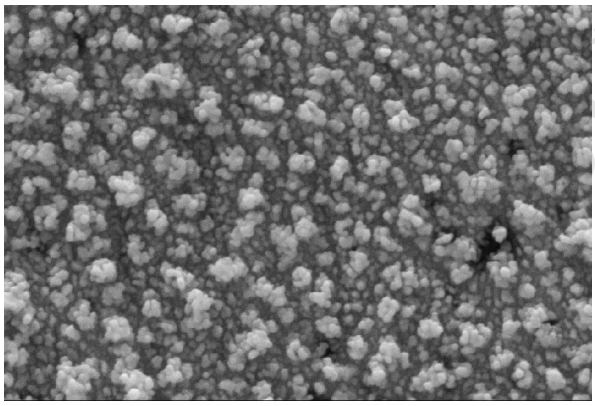
200 nm

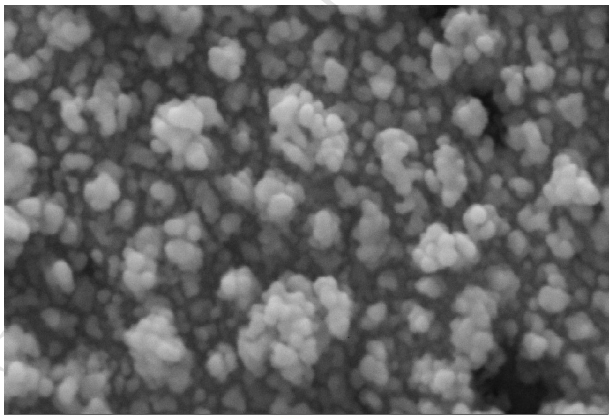
100 nm

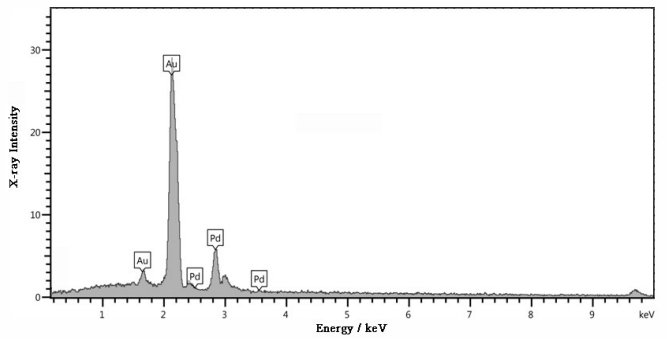
X-ray intensity
Energy / keV
Au
Au
Pd
Pd
Pd